Bryn Mawr College
Scholarship, Research, and Creative Work at Bryn Mawr College

Geology Faculty Research and Scholarship

Geology

2010

Compositions of Subsurface Ices at the Mars Phoenix Landing Site

Selby Cull
Bryn Mawr College, scull@brynmawr.edu

Raymond E. Arvidson

Michael T. Mellon

Philip Skemer

Amy Shaw

See next page for additional authors

Custom Citation

Authors
Selby Cull, Raymond E. Arvidson, Michael T. Mellon, Philip Skemer, Amy Shaw, and Richard V. Morris

Compositions of subsurface ices at the Mars Phoenix landing site

Selby Cull,[1] Raymond E. Arvidson,[1] Michael T. Mellon,[2] Philip Skemer,[1] Amy Shaw,[1] and Richard V. Morris[3]

[1] NASA's Phoenix Lander uncovered two types of ice at its 2008 landing site on the northern plains of Mars: a brighter, slab-like ice that broke during Robotic Arm operations; and a darker icy deposit. Spectra from the Phoenix Surface Stereo Imager (SSI) are used to demonstrate that the brighter material consists of nearly pure water ice, which probably formed by migration and freezing of liquid water. The darker icy material consists of $\sim$30 $\pm$ 20 wt% ice, with the remainder composed of fine-grained soil, indicating that it probably formed as pore ice. These two types of ice represent two different emplacement mechanisms and periods of deposition. **Citation:** Cull, S., R. E. Arvidson, M. T. Mellon, P. Skemer, A. Shaw, and R. V. Morris (2010), Compositions of subsurface ices at the Mars Phoenix landing site, *Geophys. Res. Lett.*, *37*, L24203, doi:10.1029/2010GL045372.

1. Introduction

[2] NASA's Mars Phoenix Lander landed on the northern plains of Mars on 25 May 2008. One of its primary objectives was to characterize the nature of shallow subsurface water ice on Mars, in an ongoing effort to understand the past and current water cycle on the planet [*Smith et al.*, 2009]. The lander was equipped with several instruments capable of characterizing the ice, including a Robotic Arm (RA) to remove overlying soil, a Wet Chemistry Laboratory (WCL) to analyze salt concentrations of the ice and soil, a Thermal and Evolved Gas Analyzer (TEGA) to analyze water concentrations and other chemical species, and a Surface Stereo Imager (SSI) to record multi-spectral observations of ice and other surface features.

[3] Over the course of the 151-sol mission, the lander dug 12 trenches (Figure 1) at the landing site [*Arvidson et al.*, 2009]. Eight of these (Dodo-Goldilocks, Upper Cupboard, Ice Man, La Mancha, Pet Donkey, Neverland, Burn Alive 3, and Snow White) exposed subsurface water ice [*Mellon et al.*, 2009].

[4] The subsurface ices fall into two distinct categories: a relatively bright ice found in the Dodo-Goldilocks and Upper Cupboard trenches (called here "Dodo-Goldilocks type ice") (Figure 2a), and a relatively dark ice found in the Snow White, Neverland, Pet Donkey, Ice Man, Burn Alive, and La Mancha trenches (called here "Snow White type ice") (Figure 2b). The two ice types had noticeably different physical properties. The formation of a sublimation lag was rapid in Snow White, relative to Dodo-Goldilocks, perhaps reflecting different soil contents available to form a lag. The Snow White ice was impossible for the RA to scrape because of exposure geometry, and so the material's hardness cannot be compared to Dodo-Goldilocks [*Arvidson et al.*, 2009; *Shaw et al.*, 2009]. The RA used its backhoe on Dodo-Goldilocks, chipping off several large chunks of ice from the trench, indicating that Dodo-Goldilocks was easily fractured and likely in slab form. The inferred differences in the physical properties of the two types of ice suggest that they may have different formation and/or evolutionary histories, as proposed by *Mellon et al.* [2009]; however, because the RA did not perform the same types of digs on both ices, their physical properties cannot be compared directly.

[5] Several mechanisms have been proposed for the origin of subsurface ice in the Martian northern plains. Based on thermal modeling and ice depth estimates from the Gamma Ray Spectrometer (GRS) aboard Mars Odyssey, *Mellon et al.* [2004] concluded that, on a regional scale, the subsurface ice is in diffusive equilibrium with water vapor in the atmosphere, suggesting that the subsurface ice must be pore ice that was emplaced by vapor diffusion and condensation. Others have proposed that the subsurface ice may more closely resemble relatively-pure massive ice that was originally emplaced by freezing of a body of surface water (e.g., a lake or ocean) [*Carr et al.*, 1990], accumulation and burial of packed snow during periods of high obliquity [e.g., *Mischna et al.*, 2003], or buried glaciers [*Prettyman et al.*, 2004].

[6] One of the most important criteria for distinguishing between these two categories of ice formation (pore ice versus pure massive ice) is the ice:soil ratio of the layer. For massive ice, the ice:soil ratio should be high, assuming that the original ice was contaminated by only small amounts of soil or dust. For pore ice, the ice:soil ratio should be low, the exact ratio being limited by the available pore space within the original soils.

[7] In this study, we use spectra from the SSI instrument to estimate the ice:soil ratio in the two types of subsurface ice observed at the Phoenix landing site. We first model the photometric functions of the two types of ices. We then use a non-linear mixing model to estimate contributions of ice and soil to the SSI spectra. Finally, we estimate the weight percent of soil present in each type of ice, with an eye toward understanding their different formation histories.

2. Methods

[8] The SSI is a stereo imager with 12-position filter wheels at 13 unique wavelengths from 0.445 μm to 1.001 μm [*Smith et al.*, 2009]. To estimate the ratio of ice to soil in the two types of ices, we compare SSI spectra to model spectra produced using a non-linear mixing model. The SSI spectra

[1]Department of Earth and Planetary Sciences, Washington University in St. Louis, St. Louis, Missouri, USA.
[2]DEPARTMENT XXX, University of Colorado at Boulder, Boulder, Colorado, USA.
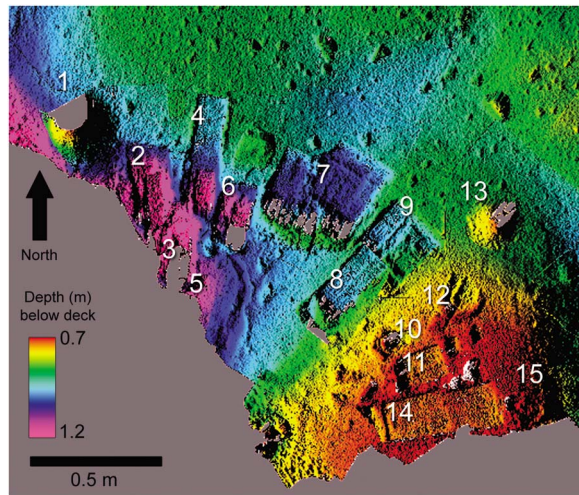[3]NASA Johnson Space Center, Houston, Texas, USA.

Figure 1. The workspace at the Phoenix landing site, with depth below deck calculated from SSI stereo pairs [*Mellon et al.*, 2009]. The lander excavated 12 trenches and produced three dump piles along its northeast side (right): Caterpillar Dump Pile (1), Dodo-Goldilocks trench (2), Stone Soup trench (3), Upper Cupboard trench (4), Lower Cupboard trench (5), Ice Man trench (6), La Mancha trench (7), Neverland trench (8), Pet Donkey trench (9), Bear's Lodge trench (10), Burn Alive 3 trench (11), Runaway trench (12), Bee Tree dump pile (13), Snow White trench (14), and Croquet Ground dump pile (15).

were 5x5 pixel averages chosen to be representative of the ices examined. The model spectra are calculated as

$$r(i,e,g) = \frac{w}{4\pi}\frac{\mu_0}{\mu_0+\mu}\{p(g) + H(\mu_0)H(\mu) - 1\}K \qquad (1)$$

where $r(i, e, g)$ is the bidirectional reflectance; i, e, and g are the incidence, emergence, and phase angles, respectively; w is the single-scattering albedo, μ_0 is the cosine of i, μ is the cosine of e, $p(g)$ is the surface phase function, $H(\mu_0)$ $H(\mu)$ describe multiple scattering, and K describes the porosity of the material [*Hapke*, 1993, 2008].

[9] The single-scattering albedos of mixtures of ice and soil were calculated from *Hapke* [1993] as

$$w = \frac{\sum_{i=1}^{i=n}(Q_{Si}M_i/\rho_i D_i)}{\sum_{i=1}^{i=n}(Q_{Ei}M_i/\rho_i D_i)} \qquad (2)$$

where M_i is the mass fraction of component i, ρ_i the solid density, D_i the grain diameter, Q_{Si} the scattering efficiency, Q_{Ei} the extinction efficiency, and the summation is carried out for all components in the mixture. Two components were considered: soil and water ice. Secondary phases (e.g., perchlorate) might be present, but will only begin to affect spectral signatures at high mass fractions (>10 wt% for perchlorate) [*Cull et al.*, 2010b]. Because Phoenix detected only small fractions of these (0.4–0.6 wt% for perchlorate) [*Hecht et al.*, 2009], we exclude them from our spectral modeling.

[10] The scattering and extinction efficiencies were calculated as described by *Roush* [1994], a procedure which requires optical constants for both components. The soil

component utilized optical constants based on a Mauna Kea palagonite sample: a low-temperature alteration product of fine-grained basaltic ash [*Clancy et al.*, 1995]. Based on orbital observations from the Compact Reconnaissance Imaging Spectrometer for Mars, dehydrated palagonite mixed with nanophase iron oxides accurately predicts the grain sizes observed at the Phoenix landing site [*Cull et al.*, 2010a], although it produces a poor fit at lower wavelengths. Optical constants for ice were used from *Warren* [1984]. Solid densities of $\rho = 0.9167$ g/cm^3 and $\rho = 2.700$ g/cm^3 [e.g., *Allen et al.*, 1997] were used for water ice and palagonite, respectively. The soil grain size was assumed to be ~60 micrometers, based on observations from Phoenix's Optical Microscope [*Goetz et al.*, 2010]. This leaves the spectrum dependent only on the relative amounts of ice and soil in each spectrum, the ice grain size, and the porosity of the material.

[11] *Moore et al.* [1987] estimated that soils at the Viking landing sites had porosities varying between 25 and 60%. *Zent et al.* [2010] estimated a porosity for Phoenix surface soils between 50 and 55%, based on heat capacity measurements. For the sake of modeling, we restrict porosities of Phoenix materials to 25 to 60%; however, we find that porosity has a negligible effect on our mixtures.

[12] To estimate the ice grain size parameter, we ran two types of models: one assuming the ice was in massive form, and one assuming pore ice. For pore ice, the ice grain sizes were assumed to be no larger than the pore space within the soil. For massive ice, "grain size" is actually representing path length through a single ice crystal before being refracted at the crystal boundary, and was defined as being between 0.1 μm and 1 cm: the lower and upper limits expected for subsurface ice.

[13] The surface phase function was modeled as a single-lobed Henyey-Greenstein model [*Henyey and Greenstein*, 1941]:

$$p(g) = \frac{(1-\delta^2)}{(1 + 2\delta\cos(g) + \delta^2)^{3/2}} \qquad (3)$$

where δ is an asymmetry factor constrained to be between -1 and 1 ($\delta = 0$ for isotropic scatter). The asymmetry factor
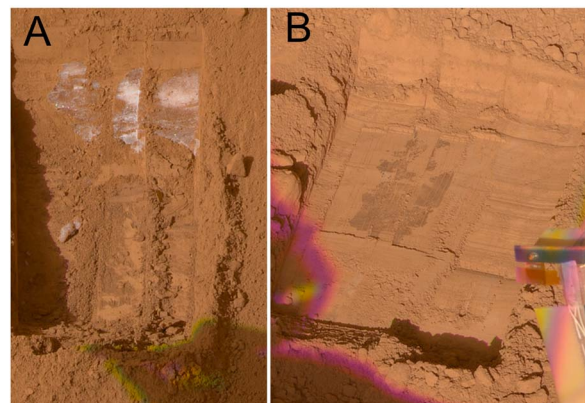

Figure 2. SSI images of the two types of ice. (a) The Dodo-Goldilocks trench at the Phoenix landing site. The light-toned material in the trench is water ice, confirmed by SSI spectra. (b) The Snow White trench. The dark material in the trench bottom is water ice, confirmed by TEGA analysis.
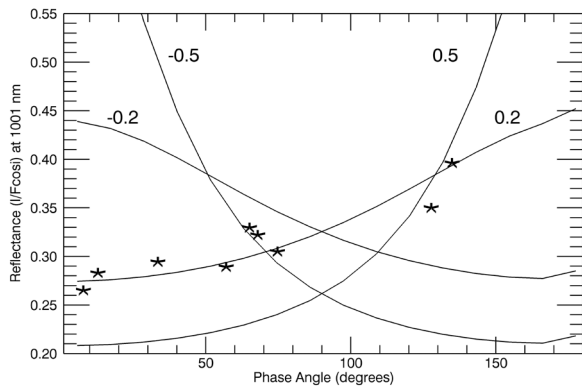
Figure 3. Comparing scattering behavior at the Snow White trench (red stars) to calculated phase functions from equation (2) (lines). The Snow White ice is clearly forward-scattering, with a best-fit asymmetry parameter of ~0.15.

for Snow White ice was calculated using multiple observations of ices exposed less than two hours previously, taken at varying phase angles (Figure 3). The brightness of each observation at 1.001 μm (a relatively noise-free band) was plotted against phase angle and fit to model results of varying δ values. The asymmetry factor could not be found for Dodo-Goldilocks, because it lacked a wide enough range of phase angle observations.

3. Results

[14] Because the asymmetry factor (δ) for the Dodo-Goldilocks ice could not be determined, the model contained too many unconstrained parameters, and an exact ice:soil ratio could not be determined. However, because Dodo-Goldilocks ices have a strong water ice-induced slope at 1.001 μm, modeling can be used to estimate the ice:soil ratio (Figure 4a). The modeling shows that soil dominates the spectrum at all wavelengths, and even a small amount of

soil mixed with ice is capable of masking the water ice signature. Any ice-soil mixture with >1 wt% soil masks the 1.001 μm absorption; hence, Dodo-Goldilocks must be at least 99 wt% pure water ice.

[15] The δ factor was calculated for the Snow White type ice (Figure 3). The scattering behavior was best fit by δ=0.15, a moderately forward-scattering material. Of the two types of models run – pore ice vs. massive ice – the Snow White ice was poorly fit by massive ice and well fit by pore ice (Figure 4b). Massive ice, with its higher ice:soil ratio and larger ice grain sizes, produced a spectrum that was too bright to fit the Snow White ice.

[16] Because soil dominates the spectrum in this wavelength region, an exact ice:soil ratio could not be obtained for the Snow White ices. However, by matching the overall albedo of the spectrum, we were able to place an upper limit on the ice fraction in the material. The Snow White ice spectrum albedo was best fit by a model that included ~30 ± 20 wt% ice, as shown in Figure 4b. Albedo at 0.445 μm is not well fit by this model; however, this poor fit was expected because the analog we use for soil does not perfectly fit Phoenix soils at very short wavelengths [*Cull et al.*, 2010a].

4. Discussion

[17] Although modeling was unable to produce exact ice:soil ratios, it has constrained the ice fraction in both the Dodo-Goldilocks and Snow White types of ice. Because the 1.001 μm slope is not masked in Dodo-Goldilocks ices, Dodo-Goldilocks must be at least 99wt% pure water ice. The Snow White ices are estimated to have <50 wt% ice, with a best fit of ~30 ± 20 wt% ice. These estimates are consistent with other Phoenix observations: ~30 wt% ice is ~55 vol.% ice, which is consistent with Thermal and Electrical Conductivity Probe (TECP) estimates of 50–55% porosity for average ice-free soils derived from measured heat capacity [*Hudson et al.*, 2009; *Zent et al.*, 2010]. If ice were to diffuse into this soil, filling the pore space, it would represent ~50–55 vol.% of the mixture.

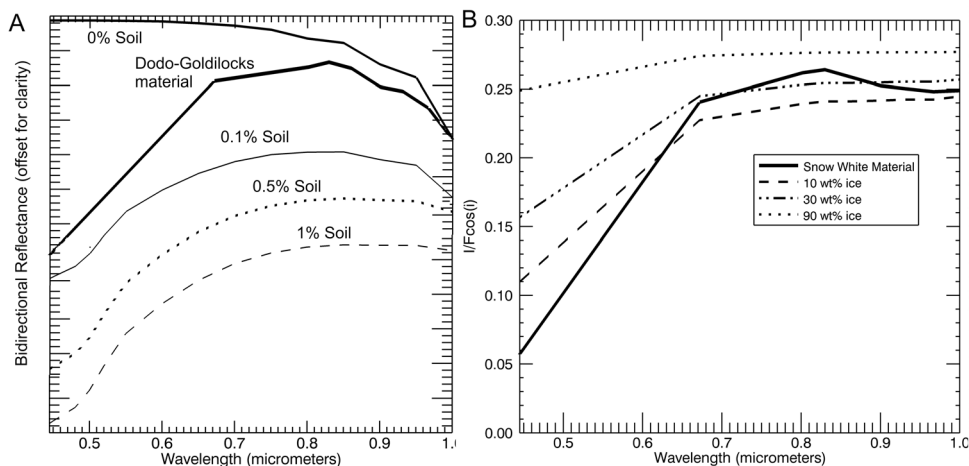**Figure 4.** (a) Comparing 1.001 μm band depths in various model results. Any composition with >1 wt% soil masks the 1.001 μm absorption, illustrating that Dodo-Goldilocks must be at least 99wt% pure water ice. (b) Freshly exposed (<2 hours old) ice at the Snow White trench (thick line) vs. model results of ice-soil mixtures. The shorter wavelengths do not fit the observed spectrum; however, this is expected due to the soil analog used in the model. The overall albedo and shape of the longer wavelengths is the basis for our interpretation of 30 wt% +/− 20 wt %".

[18] These results have important implications for our understanding of subsurface ice at the Phoenix landing site. It is likely that the two ices were emplaced via different mechanisms. The pore ice observed in Snow White is probably the result of vapor diffusion through the overlying soil layer and condensation of pore ice in the cold soil subsurface, as proposed by *Mellon et al.* [2004]. This type of ice is the dominate form, found at 90% of trenched ice exposures [*Mellon et al.*, 2009]. The relatively-pure, light-toned ice typified at Dodo-Goldilocks, on the other hand, represents a concentrated deposition of ice. This light-toned ice may have formed from a buried surface ice, such as snow; however, supraposed decimeter-scale surface rocks argue for an in-situ formation mechanism, such as ice lenses or needle ice (see *Mellon et al.* [2009] for a detailed discussion). It is likely that an in-situ formation would involve the migration of thin films of adsorbed water, a phenomenon that appears to be active at the Phoenix landing site, based on concentrated patches of perchlorate salts [*Cull et al.*, 2010b].

[19] Our spectral analysis supports the contention that these two ice deposits exhibit distinct concentrations and formed by different mechanisms. The presence of these two types of ice within the relatively small sample space of the Phoenix lander implies that both emplacement mechanisms are common throughout the northern plains. Moreover, the lack of gradation between the two types of ices suggests two different periods of emplacement.

5. Conclusions

[20] We conclude that the two types of ices exposed at the Mars Phoenix landing site are both physically and compositionally distinct. The Snow White type ice is best modeled as 30 ± 20 wt% ice, indicating that it is probably pore ice trapped between grains of soil. The Dodo-Goldilocks ice, on the other hand, is >99% pure water ice, with only a small amount of dust present. These two distinctly different compositions point to different formation mechanisms and/or subsequent evolutions of these two ices.

References

Allen, C. C., R. V. Morris, D. J. Lindstrom, M. M. Lindstrom, and J. P. Lockwood (1997), JSC Mars-1 – Martian regolith stimulant, *Lunar Planet. Sci.*, *XXVIII*, Abstract 1797.

Arvidson, R. E., et al. (2009), Results from the Mars Phoenix Lander Robotic Arm experiment, *J. Geophys. Res.*, *114*, E00E02, doi:10.1029/2009JE003408, [printed *115*(E1), 2010].

Carr, M., et al. (1990), D/H on Mars: Effects of floods, volcanism, impacts, and polar processes, *Icarus*, *87*, 210–227, doi:10.1016/0019-1035(90)90031-4.

Clancy, R. T., S. W. Lee, G. R. Gladstone, W. W. McMillan, and T. Rousch (1995), A new model for Mars atmospheric dust based upon analysis of ultraviolet through infrared observations from Mariner 9, Viking, and Phobos, *J. Geophys. Res.*, *100*, 5251–5263, doi:10.1029/94JE01885.

Cull, S., R. E. Arvidson, M. Mellon, S. Wiseman, R. Clark, T. Titus, R. V. Morris, and P. McGuire (2010a), Seasonal H_2O and CO_2 ice cycle at the Mars Phoenix landing site: 1. Prelanding CRISM and HiRISE observations, *J. Geophys. Res.*, *115*, E00D16, doi:10.1029/2009JE003340.

Cull, S., et al. (2010b), Concentrated perchlorate at the Mars Phoenix landing site: Evidence for thin film liquid water on Mars, *Geophys. Res. Lett.*, *37*, L22203, doi:10.1029/2010GL045269.

Goetz, W., et al. (2010), Microscopy analysis of soils at the Phoenix landing site, Mars: Classification of soil particles and description of their optical and magnetic properties, *J. Geophys. Res.*, *115*, E00E22, doi:10.1029/2009JE003437.

Hapke, B. (1993), *Theory of Reflectance and Emittance Spectroscopy*, Cambridge Univ. Press, Cambridge, U.K., doi:10.1017/CBO9780511524998.

Hapke, B. (2008), Bidirectional reflectance spectroscopy: 6. Effects of porosity, *Icarus*, *195*, 918–926, doi:10.1016/j.icarus.2008.01.003.

Hecht, M. H., et al. (2009), Detection of perchlorate and the soluble chemistry of Martian soil at the Phoenix Lander site, *Science*, *325*, 64–67, doi:10.1126/science.1172466.

Henyey, L. G., and J. L. Greenstein (1941), Diffuse radiation in the galaxy, *Astrophys. J.*, *93*, 70–83, doi:10.1086/144246.

Hudson, T. L., O. Aharonson, and N. Schorghofer (2009), Laboratory experiments and models of diffusive emplacement of ground ice on Mars, *J. Geophys. Res.*, *114*, E01002, doi:10.1029/2008JE003149.

Mellon, M., et al. (2004), The presence and stability of ground ice in the southern hemisphere of Mars, *Icarus*, *169*, 324–340, doi:10.1016/j.icarus.2003.10.022.

Mellon, M., et al. (2009), Ground ice at the Phoenix landing site: Stability state and origin, *J. Geophys. Res.*, *114*, E00E07, doi:10.1029/2009JE003417, [printed *115*(E1), 2010].

Mischna, M. A., M. I. Richardson, R. J. Wilson, and D. J. McCleese (2003), On the orbital forcing of Martian water and CO_2 cycles: A general circulation model study with simplified volatile schemes, *J. Geophys. Res.*, *108*(E6), 5062, doi:10.1029/2003JE002051.

Moore, H. J., et al. (1987), Physical properties of the surface materials at the Viking landing sites on Mars, *U.S. Geol. Surv. Prof. Pap.*, *1389*.

Prettyman, T. H., et al. (2004), Composition and structure of the Martian surface in the high southern latitudes from neutron spectroscopy, *J. Geophys. Res.*, *109*, E05001, doi:10.1029/2003JE002139.

Roush, T. (1994), Charon: More than water ice?, *Icarus*, *108*, 243–254, doi:10.1006/icar.1994.1059.

Shaw, A., R. E. Arvidson, R. Bonitz, J. Carsten, H. U. Keller, M. T. Lemmon, M. T. Mellon, M. Robinson, and A. Trebi-Ollennu (2009), Phoenix soil physical properties investigation, *J. Geophys. Res.*, *114*, E00E05, doi:10.1029/2009JE003455, [printed *115*(E1), 2010].

Smith, P., et al. (2009), H_2O at the Phoenix landing site, *Science*, *325*, 58–61.

Warren, S. G. (1984), Optical constants of ice from the ultraviolet to the microwave, *Appl. Optics*, *23*, 1206–1225.

Zent, A. P., M. H. Hecht, D. R. Cobos, S. E. Wood, T. L. Hudson, S. M. Milkovich, L. P. DeFlores, and M. T. Mellon (2010), Initial results from the thermal and electrical conductivity probe (TECP) on Phoenix, *J. Geophys. Res.*, *115*, E00E14, doi:10.1029/2009JE003420.

R. E. Arvidson, S. Cull, A. Shaw, and P. Skemer, Department of Earth and Planetary Sciences, Washington University in St. Louis, St. Louis, MO 63130, USA.

M. T. Mellon, DEPARTMENT, Campus Box 392, University of Colorado at Boulder, Boulder, CO 80309, USA.

R. V. Morris, NASA Johnson Space Center, Houston, TX 77058, USA.